BESSM, 2023, Vol 7, No 1, 32-37
https://doi.org/10.54987/bessm.v7i1.900

HIBISCUS PUBLISHER

BULLETIN OF ENVIRONMENTAL SCIENCE & SUSTAINABLE MANAGEMENT

Website: http://journal.hibiscuspublisher.com/index.php/BESSM/index

BESSM VOL 7 NO 1 2023 Azokeratin

Pseudomonas sp. strain Neni-12 Growth on Acrylamide Exhibit Substrate Inhibition

Rusnam[1]* and Umar Abubakar Muhammad[2]

[1]Department of Agricultural Engineering, Faculty of Agricultural Technology, Andalas University, Padang, 25163, Indonesia.
[2]Department of Biological Sciences, Faculty of Science, Gombe State University, P.M.B 127, Tudun Wada, Gombe, Gombe State, Nigeria.

*Corresponding author:
Prof Dr Rusnam,
Department of Agricultural Engineering,
Faculty of Agricultural Technology,
Andalas University,
Padang, 25163,
Indonesia.
Email: rusnam_ms@yahoo.com

HISTORY

Received: 3rd June 2023
Received in revised form: 24th July 2023
Accepted: 30th July 2023

KEYWORDS

Acrylamide-degrading
Pseudomonas sp.
Bioremediation
Haldane
Substrate inhibition kinetics

ABSTRACT

The bacterium *Pseudomonas* sp. strain Neni-12 isolated from volcanic soil showed the ability to grow on high concentrations of acrylamide. The acrylamide-degrading bacterium grew best in the presence of glucose with acrylamide as the sole nitrogen source. The inhibitory effects of acrylamide as a substrate for growth of this bacterium on the growth rate was modelled using several secondary models such as Haldane, Monod, Moser, Webb, Teissier (Tessier), Han-Levenspiel, Yano-Koga, Aiba, Luong, Webb and Hinshelwood. The models Luong and Han-Levenspiel failed to fit the data. The statistical analysis and accuracy of the all six kinetic models used indicated that Haldane was the best model with small values for RMSE and AICc, adjusted R^2 values, F-test and with Bias Factor and Accuracy Factor nearest to unity (1.0). The Haldane's constants: maximal growth rate, half-saturation constant for maximal growth and half-inhibition constant symbolized by μ_{max}, K_s, and n were 1.637 h^{-1} (95% C.I., 1.297 to 1.978), 210.99 mg/L (95% C.I., 135.01 to 286.97), 5198 mg/L (95% C.I., 4642 to 5755) and 545.68 (95% C.I., 389.94 to 701.43), respectively. The model's parameter obtained in this study will be very useful in future scale-up macrocosm studies.

INTRODUCTION

Environmental issues are increasing rapidly as thousands of various hazardous chemicals are released every day as a result of human activities. Demands are widely pursued for safe and controllable environmentally pollutant alternatives with reduced environmental impact [1]. Acrylamide (CH_2=CHCONH$_2$) is an amide group consisting of three-carbon compound with an α, β-unsaturated olefin bond. This compound is used to make polymers, particularly polyacrylamide, as a commercial conjugated reactive molecule [2–4]. Acrylamide is used as a binding, thickening and flocculating agent worldwide in the industry. [5,6]. Acrylamide is also used to stop soil erosion and in wastewater disposal systems, as pesticide ingredients, cosmetics products, sugar processing. The repeated use of acrylamide and polymers (polyacrylamide) pollute ground and sea [2,3]. Acrylamide is a rising dangerous pollutant. Acrylamide enters the body via ingestion, the skin, lungs and digestive tract [7]. Human reaction to acrylamide is primarily via its exposure to skin impacting the monomer acrylamide and of respiratory dust and vapor. Acrylamide is a recognized mammalian neurotoxicant, carcinogen and terratogen [5]. Acrylamide exerts its toxic effect when it is oxidized to the epoxide glycidamide that catalyzed by an enzymatic reaction involving cytochrome P450 2E1[8]. Previous experiments also shown that acrylamide in animal and plant cells and its oxidized type glycidamide also induced abnormalities. [9]. Given that acrylamide is harmful to human health, it must be eliminated from the atmosphere. Previously, several microorganisms such as *Pseudomonas* sp. [10], *Pseudomonas stutzeri* [11], *Pseudonocardia thermophila* [12], *Bacillus cereus* [13], the fungi *Aspergillus oryzae* [14] and yeast (KCTC 11960BP) [15].

Lately, many statistical models have been used to describe the synthesis of compounds in the natural world which are exposed to microbial communities. Monod is one of the most often used mathematical equations in defining the use of substrates related to growth rate [16]. The restriction of this approach is it is not able to cater for substrate inhibition to the rate. Due to this, other models such as Haldane or other inhibitory models was built on this basis including Aiba, Webb (Edward), Teissier Yano and Koga, Hans-Levenspiel and Luong [17,18]. Hence, the utilization of considerable models available could replace the Haldane in some circumstances and discloses

mechanistic process. To date, limited statistical tests were used to accept the best model in modelling the kinetics of xenobiotics biodegradation, and the most commonly used test is the coefficient of determination (R^2) [19,20]. However, by using this coefficient of determination (R^2), the number of parameters used in the model needs to be adjusted [21–23]. This adjustment can be made using an adjusted coefficient of determination (adjR^2), root mean square error RMSE, Corrected Akaike Information Criteria (AICc) and others. In this present study the growth rate on acrylamide was studied using various kinetic models.

MATERIALS AND METHODS

Growth and maintenance of acrylamide-degrading bacterium

Pseudomonas sp. strain Neni-12 was isolated from volcanic soil [24] and was maintained in minimal salts medium (MSM). The bacterium was initially able to grow only at 1000 mg/L, but several serial transfer processes under increasing acrylamide concentrations allows the bacterium to tolerate nearly 5000 mg/L acrylamide (results published elsewhere).

The MSM (pH 7.5) with glucose autoclaved separately is composed of (per liter): 6.8 g of KH_2PO_4 (R & M Chemicals, Selangor, Malaysia), 10 g of glucose as the sole carbon source (Spectrum Chemicals, Malaysia Sdn. Bhd), 0.005 g of $FeSO_4 \cdot H_2O$ (R & M Chemicals, Selangor, Malaysia), 0.5 g of $MgSO_4 \cdot 7H_2O$ (R & M Chemicals, Selangor, Malaysia), various concentrations of acrylamide as the sole nitrogen source with 1 mL of the following trace elements (per liter): 0.003 g of $CoCl_2 \cdot 6H_2O$, 0.01 g of $Cu(CH_3COO)_2.H_2O$ 0.03 g of $ZnCl_2$ (R & M Chemicals, Selangor, Malaysia); 0.002 g of $FeCl_2 \cdot 6H_2O$ (R & M Chemicals, Selangor, Malaysia) and 0.05 g of H_3BO_3 (JT Baker, John Townsend Baker, Phillipsburg, N.J., U.S.A.).

In order to avoid degradation via heating, acrylamide was sterilized by passing through a 0.45 µm polytetrafluoroethylene (PTFE) syringe filter (. The culture was incubated on a shaking incubator (Certomat R, USA) at 15 ºC at 150 rpm for 96 h [25]. Growth was monitored as an increase in absorbance at 600 nm using appropriate serial dilution of culture periodically sampled from the flask.

Growth kinetics on acrylamide

The bacterial growth kinetics on acrylamide was studied using a batch culture of the bacterium supplemented with acrylamide at concentrations of up to 5000 mg/L. The modified Gompertz model was utilised in the primary inhibition kinetics modelling to obtain the growth parameter maximum specific growth rate or μ_m. The equation is as follows;

$$y = A\exp\left\{-\exp\left[\frac{\mu_m e}{A}(\lambda - t) + 1\right]\right\} \quad (1)$$

The values obtained from this primary modelling exercise (published elsewhere) was then used to model various growth kinetics model as follows;

Table 1. Kinetic models for growth of bacterium on acrylamide.

Author	Degradation Rate	Author
Monod	$\frac{\mu_{max} S}{S + K_s}$	[26]
Haldane	$\frac{\mu_{max} S}{S + K_s + \left(\frac{S^2}{K_i}\right)}$	[27]
Teissier	$\mu_{max}\left(1 - exp\left(-\frac{S}{K_i}\right) - exp\left(\frac{S}{K_s}\right)\right)$	[28]
Aiba	$\mu_{max}\frac{S}{K_s + S} exp\left(-\frac{S}{K_i}\right)$	[29]
Yano and Koga	$\frac{\mu_{max} S}{S + K_s + \left(\frac{S^2}{K_i}\right)\left(1 + \frac{S}{K}\right)}$	[30]
Han and Levenspiel	$\mu_{max}\left(1 - \left(\frac{S}{S_m}\right)\right)^n \left(\frac{S}{S + K_s\left(1 - \left(\frac{S}{S_m}\right)\right)^m}\right)$	[31]
Luong	$\mu_{max}\frac{S}{S + K_s}\left(1 - \left(\frac{S}{S_m}\right)\right)^n$	[32]
Moser	$\frac{\mu_{max} s^n}{K_s + s^n}$	[33]
Webb	$\frac{\mu_{max} S\left(1 + \frac{S}{K}\right)}{S + K_s + \frac{S^2}{K_i}}$	[34]
Hinshelwood	$\mu_{max}\frac{S}{K_s + S}(1 - K_p P)$	[35]

Note:
μ_{max} maximal specific growth rate
K_s half saturation constant
K_i inhibition constant
S_m maximal concentration of substrate tolerated
K_p product inhibition constant
m, n, K curve parameters
S substrate concentration
p product concentration

Fitting of the data

Nonlinear regression was carried out using the CurveExpert Professional software (Version 1.6), which utilizes the Marquardt algorithm to fit the Gompertz and several inhibition kinetics models (**Table 1**) by nonlinear regression. This algorithm reduces the sums of squares of the residuals.

Statistical analysis

The following statistical functions were utilized to determine the best models;

The RMSE allows number of parameters' penalty and was calculated using Equation 1, where n illustrates the number of experimental data, where else p is the number of parameters calculated by the model and experimental data and values predicted by the model are Ob_i and Pd_i, respectively [36]. With the regression line approaching the data points, the root mean square error (RMSE) reduces due to the reduced error in the model. More accurate predictions are generated by a model that has a lower error rate.

Comparable in magnitude to the dependent (outcome) variable, the RMSE values span an infinite number of positive infinities. The root mean square error (RMSE) can be employed to assess the extent of imprecision in a statistical model, including regression models. If a value is zero, it signifies that the predicted and actual values are an exact match. The model exhibits superior data fit and generates more precise predictions, as indicated by low RMSE values. In contrast, increased levels indicate a greater magnitude of errors and a reduced number of precise predictions.

$$RMSE = \sqrt{\frac{\sum_{i=1}^{n}(Pd_i - Ob_i)^2}{n-p}} \quad \text{(Eqn. 1)}$$

The R^2 value, also known as the coefficient of determination, was used in linear regression to select the model that provided the best fit. On the other hand, in the case of nonlinear regression, the R^2 does not provide a comparative analysis in situations in which the number of parameters in the various models varies. In order to get around this obstacle, the quality of the nonlinear models was determined by adjusting the R^2 value. S_y^2 is the total variance of the y-variable, while RMS stands for residual mean square. These two terms are used in the adjusted R^2 formula (Equations 2 and 3).

$$Adjusted\ (R^2) = 1 - \frac{RMS}{S_Y^2} \quad \text{(Eqn. 2)}$$

$$Adjusted\ (R^2) = 1 - \frac{(1-R^2)(n-1)}{(n-p-1)} \quad \text{(Eqn. 3)}$$

One can measure the relative quality of various statistical models for a given set of experimental data by using the Akaike Information Criterion (AIC). This criterion was developed by Akaike. Instead, data sets that have a large number of parameters or few values should utilize the AIC that has been corrected, which is denoted by the letter AICc [37]. The AICc was determined using the equation that is presented below (Equation 4).

$$AICc = 2p + n1n\left(\frac{RSS}{n}\right) + 2(p+1) + \frac{2(p+1)(p+2)}{n-p-2} \quad \text{(Eqn. 4)}$$

Another statistical measure that is founded on information theory is known as the Bayesian Information Criterion (BIC) (Equation 5), which can be compared to the AICc. Models with the lowest Bayesian information criterion (BIC) are typically preferred over those with higher BICs when choosing from a finite number of models. It has close ties to the Akaike information criteria and is partially based on the likelihood function (AIC). This error function imposes a harsher penalty on the number of parameters than the AIC does [38].

$$BIC = n.\ln\frac{RSS}{n} + p.\ln(n) \quad \text{(Eqn. 5)}$$

The Hannan–Quinn information criterion, often known as the HQC, is an additional error function approach that is based on the information theory (Equation 7). To evaluate how well a statistical model fits data, experts use the Hannan-Quinn information criterion (HQC). It is a common metric to employ when choosing one model over another. In contrast to the LLF, it is connected to Akaike's information criterion. The HQC, like the AIC, includes a penalty function for the total number of model parameters, however it is significantly bigger than the value assigned by the AIC because the equation contains the *ln ln n* term [39];

$$HQC = n \times ln\frac{RSS}{n} + 2 \times p \times ln(\ln n) \quad \text{(Eqn. 7)}$$

Both BF and AF were utilized in an effort to evaluate the appropriateness of the models. In order to get a correlation of 1 between the anticipated value and the observed value, the Bias Factor needs to be equal to 1. The Bias Factor and Accuracy Factor originates from predictive microbiology under the food microbiology field and have found applications in modelling microbial growth that leads to food spoilage [40–47]. A fail-safe model is indicated when the value of the Bias Factor (Equation 8) is greater than 1, and a fail-negative model is indicated when the value of the Bias Factor is less than 1. When compared to 1, a value of Accuracy that is less than 1 indicates a less accurate prediction (Equation 9).

$$Bias\ factor = 10\left(\sum_{i=1}^{n} log\frac{(Pd_i/Ob_i)}{n}\right) \quad \text{(Eqn. 8)}$$

$$Accuracy\ factor = 10\left(\sum_{i=1}^{n} log\frac{|(Pd_i/Ob_i)|}{n}\right) \quad \text{(Eqn. 9)}$$

Another parameter-penalized model is MPSD. The Marquardt's percent standard deviation (MPSD). This error function distribution follows the geometric mean error which allows for the penalty to the number of parameters of a model (Equation 10).

$$MPSD = 100\sqrt{\frac{1}{n-p}\sum_{i=1}^{n}\left(\frac{Ob_i - Pd_i}{Ob_i}\right)^2} \quad \text{(Eqn. 10)}$$

where p is the number of parameters, n is the number of experimental data, Ob_i is the experimental data, and Pd_i is the value predicted by the model.

RESULTS AND DISCUSSION

Growth kinetics

The growth rate of the acrylamide-degrading bacterium on acrylamide as a nitrogen source shows maximal rate at acrylamide concentrations ranging from 100 to 1000 mg/L and also substrate inhibition to the rate with a decrease in the growth rate was observed at acrylamide concentration of 5000 mg/L.

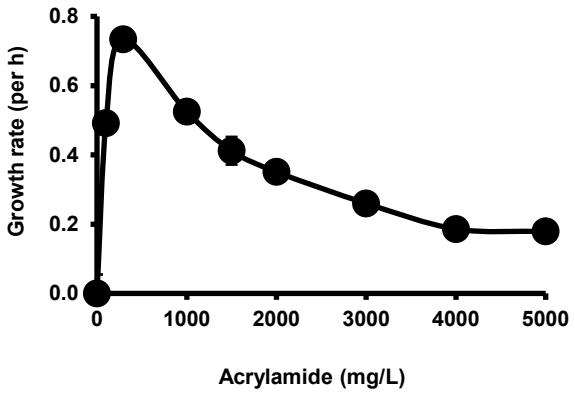

Fig. 1. Growth rate of *Pseudomonas* sp. strain Neni-12 on various acrylamide concentrations. Error bars indicate mean standard deviation (n=3).

Modelling was carried out using several other kinetic models (**Figs. 2-7**). The models Luong and Han-Levenspiel failed to fit the data. The statistical analysis and accuracy of the all six kinetic models used indicated that Haldane was the best model with small values for RMSE and AICc, adjusted R^2 values, F-test and with Bias Factor and Accuracy Factor nearest to unity (1.0) (**Table 2**). The Haldane's constants; maximal growth rate, half-saturation constant for maximal growth and half-inhibition constant symbolized by μ_{max}, K_s, and n were 1.637 h^{-1} (95% C.I., 1.297 to 1.978), 210.99 mg/L (95% C.I., 135.01 to 286.97), 5198 mg/L (95% C.I., 4642 to 5755) and 545.68 (95% C.I., 389.94 to 701.43), respectively.

The restrictions of previous models such Haldane, Andrews Noack, Web, and Yano, alternative models such as Luong, Teissier and Hans-Levenspiel were developed in that certain cases in which growth rate at very high substratum concentration became zero did not justify the use of these models [48]. To date, this is the second time that such a modelling exercise was utilized to model growth kinetics on acrylamide. Modelling the bacterial growth kinetics on toxicants is an essential part of improving successful bioremediation strategies since the obtained consistencies can be used to prepare and consider bioremediation limitations [18]. In a previous study, an acrylamide-degrading yeast shows the Luong model as the best model with the Luong's constants μ_{max}, K_s, S_m, and n (± standard error) were 0.099±0.017 hr^{-1}, 17.34 ± 5.0 mg/L, 2053.0 ±56.0 mg/L and 0.801±0.202, respectively [49].

Similarly, another acrylamide-degrading bacterium isolated from Antarctica also exhibited Luong as the best model with the half-saturation constant for maximal growth, maximal growth rate and maximal concentration of substrate tolerated and curve parameter that defines the steepness of the growth rate decline from the maximum rate symbolized by K_s, μ_{max} and S_m, and n were 18.29 mg/L (95% C.I., -17.51 to 54.10), 0.66 per day (95% C.I., 0.51 to 0.82), 5198 mg/L (95% C.I., 4642 to 5755) and 1.37 (95% C.I., 0.54 to 2.21), respectively [50].

After normalization, the specific maximal growth rate on acrylamide of the yeast fares better than the bacterium in this study suggesting a more efficient acrylamide degradation in the yeast. In contrast to yeast, this bacteria can survive in environments with much higher levels of acrylamide. Warning the u_{max} value for acrylamide obtained using curve-fitting interpolation is not the genuine value; rather, the true u_{max} should be found at the point where the gradient for the slope is zero and this value is 0.729 h^{-1} at 339 mg/L.

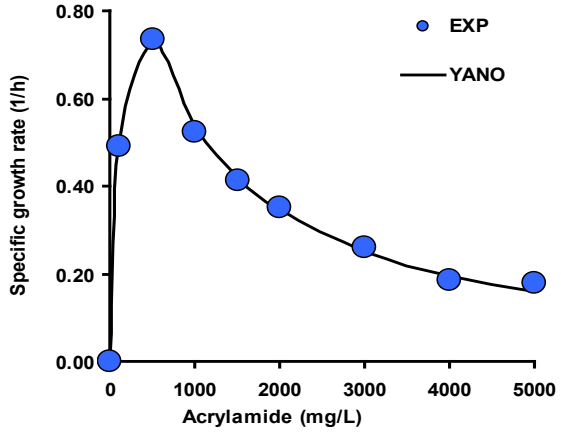

Fig. 2. Fitting of the specific growth rate of the bacterium on various concentrations of acrylamide using the Yano model.

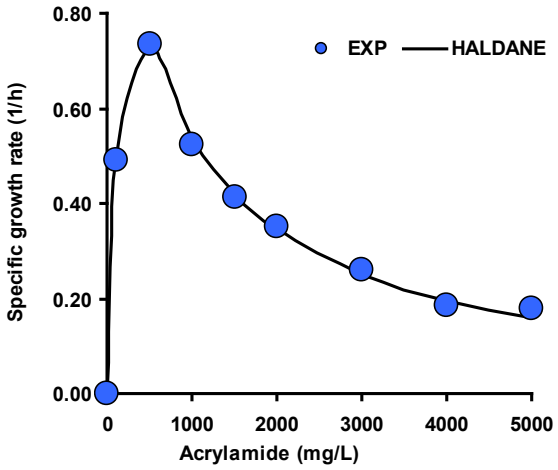

Fig. 3. Fitting of the specific growth rate of the bacterium on various concentrations of acrylamide using the Haldane model.

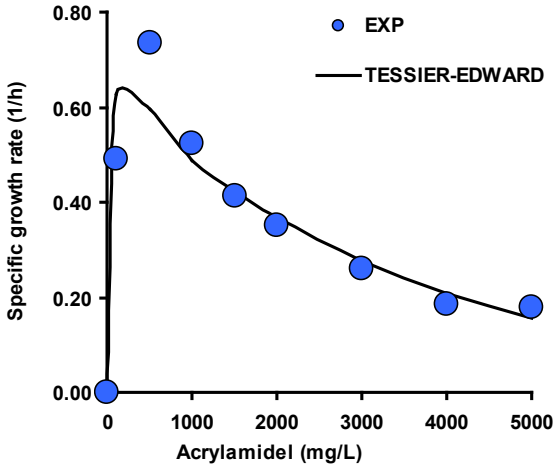

Fig. 4. Fitting of the specific growth rate of the bacterium on various concentrations of acrylamide using the Teissier model.

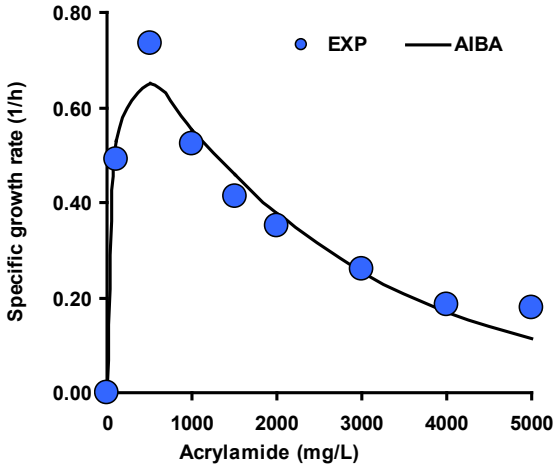

Fig. 5. Fitting of the specific growth rate of the bacterium on various concentrations of acrylamide using the Aiba model.

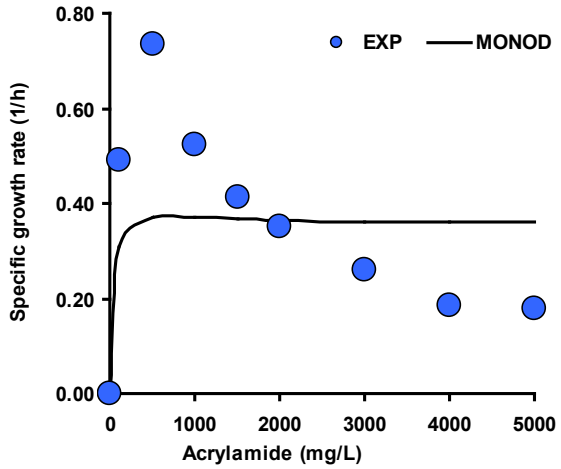

Fig. 6. Fitting of the specific growth rate of the bacterium on various concentrations of acrylamide using the Monod model.

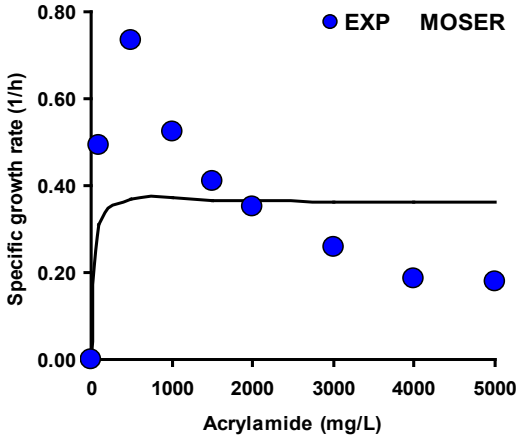

Fig. 7. Fitting of the specific growth rate of the bacterium on various concentrations of acrylamide using the Moser model.

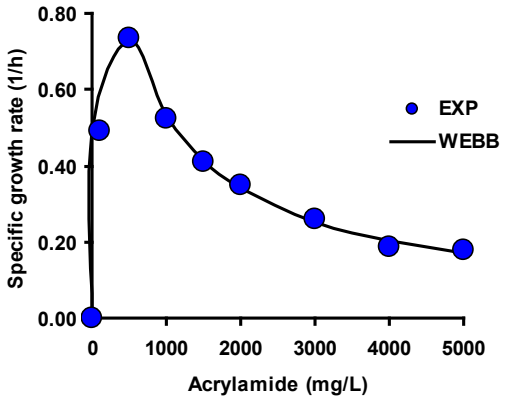

Fig. 8. Fitting of the specific growth rate of the bacterium on various concentrations of acrylamide using the Webb model.

Table 2. Statistical analysis of kinetic models.

Model	p	RMSE	adR^2	MPSD	AICc	BIC	HQC	BF	AF
Luong	4	n.a.	n.a.	n.a.	n.a.	n.a.	n.a.	n.a.	n.a.
Yano	4	0.0140	0.9951	3.449	-44.190	-73.401	-75.893	0.990	1.032
Tessier-Edward	3	0.0826	0.8108	14.480	-24.533	-41.941	-43.810	0.981	1.076
Aiba	3	0.0534	0.9310	9.198	-32.401	-49.809	-51.678	0.949	1.110
Haldane	3	0.0127	0.9961	3.149	-58.190	-75.599	-77.467	0.990	1.032
Monod	2	0.1734	-0.6556	40.605	-18.998	-29.403	-30.649	1.079	1.363
Han and Levenspiel	5	n.a.	n.a.	n.a.	n.a.	n.a.	n.a.	n.a.	n.a.
Moser	3	0.1514	0.0052	32.928	-13.625	-31.033	-32.902	1.059	1.270
Hinshlewood	4	0.2083	-2.4461	49.182	4.470	-24.741	-27.233	1.079	1.363
Webb	4	0.0107	0.9971	4.380	-48.993	-78.204	-80.695	1.001	1.023

Note:
p no of parameter
RMSE Root Mean Squared Error
R^2 Coefficient of Determination
adR^2 Adjusted Coefficient of Determination
AICC Corrected Akaike Information Criterion
BF Bias Factor
AF Accuracy Factor
n.a Not available

CONCLUSION

To conclude, the key modelling practice for the growth of this acrylamide by bacterium yields substantial real growth rates which have successfully been used with Luong as the best model in the secondary modelling exercises. The Luong's constants; maximal growth rate, half-saturation constant for maximal growth, maximal concentration of substrate tolerated and curve parameter that defines the steepness of the growth rate decline from the maximum rate symbolized by μ_{max}, K_s, S_m, and n were 0.66 per day (95% C.I., 0.51 to 0.82), 18.29 mg/L (95% C.I., -17.51 to 54.10), 5198 mg/L (95% C.I., 4642 to 5755) and 1.37 (95% C.I., 0.54 to 2.21), respectively. Acrylamide is poisonous and completely inhibits acrylamide degradation and growth on this substrate as according to the Luong model suggesting that to a certain limit, bioremediation might not be successful. To date, a simulation exercise like this has been used to model acrylamide growth kinetics.

REFERENCES

1. Vert M, Doi Y, Hellwich KH, Hess M, Hodge P, Kubisa P, et al. Terminology for biorelated polymers and applications (IUPAC Recommendations 2012). Pure Appl Chem [Internet]. 2012 Jan 11 [cited 2017 Dec 18];84(2). Available from: https://www.degruyter.com/view/j/pac.2012.84.issue-2/pac-rec-10-12-04/pac-rec-10-12-04.xml
2. Igisu H, Matsuoka M. Acrylamide Encephalopathy. Sangyo Eiseigaku Zasshi. 2002;44(2):A21.
3. Kotlova EK, Chestukhina GG, Astaurova OB, Leonova TE, Yanenko AS, Debabov VG. Isolation and primary characterization of an amidase from Rhodococcus rhodochrous. Biochem Biokhimiia. 1999 Apr;64(4):384–9.
4. Weideborg M, Källqvist T, Ødegård KE, Sverdrup LE, Vik EA. Environmental risk assessment of acrylamide and methylolacrylamide from a grouting agent used in the tunnel construction of romeriksporten, norway. Water Res. 2001 Aug;35(11):2645–52.
5. Sathesh Prabu C, Thatheyus AJ. Biodegradation of acrylamide employing free and immobilized cells of Pseudomonas aeruginosa. Int Biodeterior Biodegrad. 2007 Jan;60(2):69–73.
6. Wampler DA, Ensign SA. Photoheterotrophic Metabolism of Acrylamide by a Newly Isolated Strain of Rhodopseudomonas palustris. Appl Environ Microbiol. 2005 Oct 1;71(10):5850–7.
7. Charoenpanich J. Removal of Acrylamide by Microorganisms. In: Patil Y, editor. Applied Bioremediation - Active and Passive Approaches [Internet]. InTech; 2013 [cited 2017 Dec 18]. Available from: http://www.intechopen.com/books/applied-bioremediation-active-and-passive-approaches/removal-of-acrylamide-by-microorganisms

8. Besaratinia A, Pfeifer GP. Genotoxicity of acrylamide and glycidamide. J Natl Cancer Inst. 2004 Jul 7;96(13):1023–9.
9. Bergmark E, Calleman CJ, Costa LG. Formation of hemoglobin adducts of acrylamide and its epoxide metabolite glycidamide in the rat. Toxicol Appl Pharmacol. 1991 Nov;111(2):352–63.
10. Shukor MY, Gusmanizar N, Ramli J, Shamaan NA, MacCormack WP, Syed MA. Isolation and characterization of an acrylamide-degrading Antarctic bacterium. J Environ Biol. 2009 Jan;30(1):107–12.
11. Wang CC, Lee CM. Denitrification with acrylamide by pure culture of bacteria isolated from acrylonitrile-butadiene-styrene resin manufactured wastewater treatment system. Chemosphere. 2001 Aug;44(5):1047–53.
12. Egorova K, Trauthwein H, Verseck S, Antranikian G. Purification and properties of an enantioselective and thermoactive amidase from the thermophilic actinomycete Pseudonocardia thermophila. Appl Microbiol Biotechnol. 2004 Jul;65(1):38–45.
13. Shukor MY, Gusmanizar N, Azmi NA, Hamid M, Ramli J, Shamaan NA, et al. Isolation and characterization of an acrylamide-degrading Bacillus cereus. J Environ Biol. 2009 Jan;30(1):57–64.
14. Wakaizumi M, Yamamoto H, Fujimoto N, Ozeki K. Acrylamide degradation by filamentous fungi used in food and beverage industries. J Biosci Bioeng. 2009 Nov;108(5):391–3.
15. Rahim MBH, Syed MA, Shukor MY. Isolation and characterization of an acrylamide-degrading yeast *Rhodotorula* sp. strain MBH23 KCTC 11960BP. J Basic Microbiol. 2012;52(5):573–81.
16. Monod J. The Growth of Bacterial Cultures. Annu Rev Microbiol. 1949;3(1):371–94.
17. Gunasekaran B, Shukor MS, Masdor NA, Shamaan NA, Shukor MY. Test of randomness of residuals for the Buchanan-three-phase model used in the fitting the growth of *Paracoccus* sp. SKG on acetonitrile. J Environ Bioremediation Toxicol. 2015;3(1):12–4.
18. Halmi MIE, Shukor MS, Masdor NA, Shamaan NA, Shukor MY. Evaluation of several mathematical models for fitting the growth of sludge microbes on PEG 600. J Environ Microbiol Toxicol. 2015;3(1):1–5.
19. Motulsky HJ, Ransnas LA. Fitting curves to data using nonlinear regression: a practical and nonmathematical review. FASEB J Off Publ Fed Am Soc Exp Biol. 1987;1(5):365–74.
20. Banerjee A, Ghoshal AK. Isolation and characterization of hyper phenol tolerant *Bacillus* sp. from oil refinery and exploration sites. J Hazard Mater. 2010;176(1–3):85–91.
21. Halmi MIE, Shukor MS, Johari WLW, Shukor MY. Mathematical modeling of the growth kinetics of *Bacillus* sp. on tannery effluent containing chromate. J Environ Bioremediation Toxicol. 2014;2(1):6–10.
22. Halmi MIE, Shukor MS, Johari WLW, Shukor MY. Evaluation of several mathematical models for fitting the growth of the algae *Dunaliella tertiolecta*. Asian J Plant Biol. 2014;2(1):1–6.
23. Halmi MIE, Ahmad SA, Syed MA, Shamaan NA, Shukor MY. c*Bacillus pumilus* strain Lbna. Bull Environ Sci Manag. 2014;2(1):24–9.
24. Rusnam, Gusmanizar N. Characterization of An Acrylamide-degrading Bacterium Isolated from Volcanic Soil. J Environ Bioremediation Toxicol. 2022 Aug 5;5(1):32–7.
25. Shukor A, Yunus M, Gusmanizar N, Ramli J, Shamaan NA, MacCormack W, et al. Isolation and characterization of an acrylamide-degrading Antarctic bacterium. J Environ Biol. 2009;30(1):107–12.
26. Monod J. The Growth of Bacterial Cultures. Annu Rev Microbiol. 1949;3(1):371–94.
27. Boon B, Laudelout H. Kinetics of nitrite oxidation by Nitrobacter winogradskyi. Biochem J. 1962;85:440–7.
28. Teissier G. Growth of bacterial populations and the available substrate concentration. Rev Sci Instrum. 1942;3208:209–14.
29. Aiba S, Shoda M, Nagatani M. Kinetics of product inhibition in alcohol fermentation. Biotechnol Bioeng. 1968 Nov 1;10(6):845–64.
30. Yano T, Koga S. Dynamic behavior of the chemostat subject to substrate inhibition. Biotechnol Bioeng. 1969 Mar 1;11(2):139–53.
31. Han K, Levenspiel O. Extended Monod kinetics for substrate, product, and cell inhibition. Biotechnol Bioeng. 1988;32(4):430–7.
32. Luong JHT. Generalization of monod kinetics for analysis of growth data with substrate inhibition. Biotechnol Bioeng. 1987;29(2):242–8.
33. Moser A. Kinetics of batch fermentations. In: Rehm HJ, Reed G, editors. Biotechnology. VCH Verlagsgesellschaft mbH, Weinheim; 1985. p. 243–83.
34. Webb JLeyden. Enzyme and metabolic inhibitors [Internet]. New York: Academic Press; 1963. 984 p. Available from: https://www.biodiversitylibrary.org/bibliography/7320
35. Hinshelwood CN. The chemical kinetics of the bacterial cell. Clarendon Press, Gloucestershire, UK; 1946.
36. Wayman M, Tseng MC. Inhibition-threshold substrate concentrations. Biotechnol Bioeng. 1976;18(3):383–7.
37. Akaike H. Making statistical thinking more productive. Ann Inst Stat Math. 2010;62(1):3–9.
38. Kass RE, Raftery AE. Bayes Factors. J Am Stat Assoc. 1995 Jun 1;90(430):773–95.
39. Burnham KP, Anderson DR. Model Selection and Multimodel Inference: A Practical Information-Theoretic Approach. Springer Science & Business Media; 2002. 528 p.
40. Ross T, McMeekin TA. Predictive microbiology. Int J Food Microbiol. 1994;23(3–4):241–64.
41. Zhou K, George SM, Métris A, Li PL, Baranyi J. Lag phase of Salmonella enterica under osmotic stress conditions. Appl Environ Microbiol. 2011;77(5):1758–62.
42. Zhao J, Gao J, Chen F, Ren F, Dai R, Liu Y, et al. Modeling and predicting the effect of temperature on the growth of *Proteus mirabilis* in chicken. J Microbiol Methods. 2014;99(1):38–43.
43. Velugoti PR, Bohra LK, Juneja VK, Huang L, Wesseling AL, Subbiah J, et al. Dynamic model for predicting growth of Salmonella spp. in ground sterile pork. Food Microbiol. 2011;28(4):796–803.
44. McElroy DM, Jaykus LA, Foegeding PM. Validation and analysis of modeled predictions of growth of Bacillus cereus spores in boiled rice. J Food Prot. 2000;63(2):268–72.
45. Kowalik J, Lobacz A, Tarczynska AS, Ziajka S. Graphie validation of growth models for Listeria monocytogenes in milk during storage. Milchwissenschaft. 2012;67(1):38–42.
46. Jung SH, Park SJ, Chun HH, Song KB. Effects of combined treatment of aqueous chlorine dioxide and fumaric acid on the microbial growth in fresh-cut paprika (capsicum annuum L.). J Appl Biol Chem. 2014;57(1):83–7.
47. Huang L, Hwang CA, Phillips J. Evaluating the Effect of Temperature on Microbial Growth Rate-The Ratkowsky and a Bělehrádek-Type Models. J Food Sci. 2011;76(8):M547–57.
48. Saravanan P, Pakshirajan K, Saha P. Growth kinetics of an indigenous mixed microbial consortium during phenol degradation in a batch reactor. Bioresour Technol. 2008;99(1):205–9.
49. Othman AR, Rahim MBHA. Modelling the Growth Inhibition Kinetics of *Rhodotorula* sp. strain MBH23 (KCTC 11960BP) on Acrylamide. Bioremediation Sci Technol Res. 2019 Dec 28;7(2):20–5.
50. Syed MA, Shamaan NA, MacCormack WP, Shukor MY. Modelling the Growth Inhibition Kinetics of *Pseudomonas* sp. strain DrYJ7 on Acrylamide. Bull Environ Sci Sustain Manag. 2020 Dec 31;4(2):6–10.